

On the spectral density from instantons in quenched QCD

UKQCD Collaboration

U. Sharan, M. Teper^y

Department of Theoretical Physics, University of Oxford, Keble Road, Oxford, OX1 3NP, U.K.

Abstract

We investigate the spectral density of the Dirac operator in the background of overlapping instantons and anti-instantons. The instanton configurations are derived from SU(3) gauge field configurations at a variety of lattice spacings, volumes and cooling sweeps; and we also generate a 'gas' of instantons for purposes of comparison. We find that the spectral density appears to diverge for small eigenvalues implying that the chiral condensate diverges in quenched QCD. We show that this spectral density scales, that finite volume corrections are small and we find evidence for the screening of topological charges. However we also find that cooling alters the chiral condensate, which decreases strongly as the number of cooling sweeps increases. Thus although certain physical observables such as the topological susceptibility remain stable under cooling (and even under different cooling algorithms), this does not appear to be the case in the fermionic sector.

^xuji@thphys.ox.ac.uk^yteper@thphys.ox.ac.uk

I. INTRODUCTION

There have been a number of recent lattice calculations that attempt to determine the instanton content of the vacuum in $SU(2)$ [1] and $SU(3)$ [2,3] gauge theories. One motivation has been to make contact with phenomenological instanton models [4,5]. Another aim has been to test certain long-held theoretical ideas, such as that instantons might play an important role in chiral symmetry breaking [4,6].

To identify the instanton content of fully fluctuating vacuum gauge fields (the latter obtained from lattice Monte Carlo simulations) is far from trivial. Indeed it is not entirely clear to what extent it is either meaningful or possible. Current techniques involve smoothing the lattice gauge fields on short distances and then using some pattern recognition algorithm to resolve the topological charge density into an ensemble of overlapping (anti)instantons of various sizes and positions. At present there is only some agreement between the results of the different approximate methods being used [2,3]. Thus all these calculations should be regarded as exploratory.

In this paper we shall focus on the calculations in [3]. There the smoothing of the rough gauge fields was achieved by a process called 'cooling' [7]. This is an iterative procedure just like the Monte Carlo itself except that the fields are locally deformed towards the minimum of the action (or some variation thereof). Although some quantities, such as the topological susceptibility, are insensitive to the amount of cooling (within reason) this is not the case for the number, size distribution and density of the topological charges. Whether this leads to a real ambiguity for physical observables is an important question. It might be that the ambiguity is only apparent and that fermionic observables calculated in these cooled instanton background fields do not show much variation with cooling. For example it might be the case that the instantons that disappear with cooling are highly overlapping $Q = -1$ pairs which contribute no small modes to the Dirac operator.

One might think that the reasonable way to approach all these questions would be to perform calculations directly on the cooled lattice fields using lattice versions of the Dirac

operator. Although such explicit calculations do show that it is the instanton (would-be) zero modes that drive chiral symmetry breaking [8], one finds that lattice artefacts spoil the mixing of the instanton near-zero modes making it difficult to draw any reliable conclusions. (Although this might soon change with the implementation of domain-wall and related lattice fermions [9].)

In this paper we shall calculate the interesting low lying eigenvalue spectrum of the Dirac operator by constructing an explicit matrix representation for a given background field of overlapping instantons and anti-instantons. Given our ignorance of the full structure of the vacuum, such a method is necessarily approximate. Our approach will be to simplify the details as much as possible while still incorporating both the important symmetries of the problem and the long-distance clustering properties of an ensemble of topological charges. Our expectation is that this should ensure that our answers are qualitatively reliable [10]. Some preliminary results using this method for configurations of instantons and anti-instantons distributed at random have been given elsewhere [11,12].

Let $\lambda_n[A]$ be an eigenvalue of the Dirac operator for some given gauge field configuration A : $\delta[A]_n(x) = \lambda_n[A]_n(x)$. We know via the Atiyah-Singer Index theorem [13] that the eigenvalue spectrum will contain

$$Q[A] = n_+ - n_- \quad (1)$$

exact zero modes, where $Q[A]$ is the winding number of the gauge field configuration and n_+ are the number of zero eigenmodes with positive/negative chirality. In the chiral limit a zero eigenvalue leads to a zero determinant; so gauge field configurations with non-trivial winding number are suppressed by the light quarks of full QCD. This suppression is lost in quenched QCD where the fermion determinant is set to unity. Let $\rho(\mu; A) = \sum_n \delta(\lambda_n[A])$ be the spectral density of the Dirac operator. One can relate the chiral condensate to the spectral density via

$$h_{-} = \lim_{m \rightarrow 0} \frac{i}{\pi} \int_0^{\infty} \frac{2m - \lambda(\mu; m)}{\mu^2 + m^2} \rho(\mu; A) d\mu; \quad (2)$$

where $\bar{h}(\mu) = \lim_{V \rightarrow 1} V^{-1} h(\mu)$. Care must be taken with the limits; if we reverse the order of the limits so that we take the chiral limit in a finite box then we will see symmetry restoration [8]. This is basically due to the fact that the eigenvalue spectrum has a gap of order V^{-1} when we deal with a system with finite degrees of freedom (in our case the instantons). It is easy to see from equation (2) that the combination of the spectral gap and the absence of any exact zero modes in full QCD leads to symmetry restoration. This is however not the case in quenched QCD. In this case we still have the spectral gap but we also now have order $\frac{p}{V}$ exact zero modes, leading to $\lim_{m \rightarrow 0, V \text{ fixed}} \bar{h}_i = \frac{p}{V}$. This pathological result is well known (see for example [8,11]) and is not the main thrust of the present paper. In this paper we concentrate on the contribution of the modes which are not Atiyah-Singer exact zero modes. It is these remaining modes which will contribute when the limits are taken as in equation (2). We will therefore ignore the contribution of the exact zero modes when calculating the chiral condensate. Another subtlety in equation (2) comes from the explicit quark mass dependence of the spectral density arising from the presence of the fermion determinant in the partition function. This quark mass dependence is absent in the quenched approximation; in this latter case one may safely evaluate the limits to get

$$\bar{h}_i = i^{-}(0): \quad (3)$$

This is the Banks-Casher relation [14]. We immediately see that the low lying spectral density is crucial for this phenomenologically important condensate.

Equation (3) explains why instantons are a more interesting starting point for a discussion of chiral symmetry breaking than perturbation theory. If we neglect interactions then the perturbative vacuum becomes free. Here the spectrum grows as μ^3 . That is to say, the eigenvalues are far from zero. If on the other hand we neglect interactions amongst (anti)instantons we get an exact zero-mode for each topological charge. This contributes a term $\delta(\mu) \delta(\lambda)$. Introducing interactions will shift these distributions, but it is clear that if what one wants is a non-zero density of modes near $\lambda = 0$ then the latter approach is a more promising one than the former.

In the next section we introduce our 'toy' model for calculating the contribution of an ensemble of topological charges to the spectral density. In the following section we apply this model to the ensembles generated in [3].

II. A TOY MODEL FOR EIGENVALUE SPLITTING

We consider the case of quenched QCD (ie. the pure gauge theory). We construct a representation of the Dirac operator $\not{D}[\mathbf{A}]$ for a gauge field \mathbf{A} consisting of n_I instantons (I) and $n_{\bar{I}}$ anti-instantons (\bar{I}). Let each object have gauge field configuration A_i . We know that there are $j_{n_I} - n_{\bar{I}}$ exact zero modes, whose contribution to the spectral density we will ignore for the reasons discussed above. There are a further $n_I + n_{\bar{I}} - 2j$ "would-be zero modes"; these are the modes which would be exact zero modes if the objects were non-interacting, as in the dilute gas approximation. In an interacting system these would-be zero modes have eigenvalues split symmetrically around zero. The splitting is symmetric as non-zero eigenvalues come in pairs due to the 5 symmetry $f\not{D} = ^5g = 0$. It is these "would-be zero modes" which we expect to form that part of the low lying spectrum of the Dirac operator that is due to instantons, and so are of greatest importance in calculations of the chiral condensate.

A matrix representation is defined by $(\not{D}[\mathbf{A}])_{ji} = D_{kj} \delta_{ki}$ for some basis $f_j j_i$. It follows trivially that $D_{kj} = h_{kj} \not{D} j_i$ if the basis is orthonormal. We choose our basis to be constructed out of the would-be zero modes coming from the individual objects $f_{j_1}^+ j_1; \dots; j_{n_{\bar{I}}}^+ j_{n_{\bar{I}}}; j_1; \dots; j_{n_I}$ such that

$$\not{D}[\mathbf{A}_i] j_i = 0: \quad (4)$$

We are in effect writing the low lying eigenmodes of a given instanton configuration as a linear combination of the zero modes from the individual objects. If we were interested in the entire spectrum then we would have to include contributions from all modes but this is not necessary for our purpose. It is easy to see that

$$\begin{aligned}
h_i^+ \bar{\partial} [A] j_j^+ i &= 0 \\
h_i^+ \bar{\partial} [A] j_j^- i &= 0 \\
h_i^+ \bar{\partial} [A] j_j^- i &= V_{ij}:
\end{aligned} \tag{5}$$

The first two identities follow from the S^5 symmetry. Let us consider the third equation for a configuration consisting of a single I \bar{I} pair. The function V has, in principle, a dependence on the position of the centres of the objects (x_k), the sizes of the objects (ϵ_k) and the relative colour orientation of the two objects. We choose to ignore the colour orientation for reasons of simplicity. We can also replace the covariant derivative $\bar{\partial} [A]$ in the matrix element with $i\partial$ using the equations of motion (4). So given a trial would be zero mode wavefunction, we can actually calculate this matrix element as an overlap integral over some manifold (in all cases in this paper the manifold is simply the periodic box T^4).

$$\begin{aligned}
V_{ij} &= h_i^+ \bar{\partial} [A]_i^+ ; A_j^-] j_j^- i \\
&= h_i^+ j_i \bar{\partial} j_j^- i \\
&= V(x_i^+ ; x_i^+ ; x_j^- ; x_j^-):
\end{aligned} \tag{6}$$

Here we have assumed that the I \bar{I} gauge potential can be approximated as a sum of the individual I ; \bar{I} gauge potentials (in some appropriate singular gauge). We note that (6) will be valid for an arbitrary number of (anti)instantons if their mutual separations are large. If however we are dealing with an arbitrary configuration consisting of more than a single I \bar{I} pair, then the function V is in general unknown. It will in fact have a dependence on all the objects within the configuration through the gauge field $[A]$. We also cannot replace the covariant derivative as before. We however choose to make this replacement anyway so that (6) holds for general configurations. Again, the main justification for doing so is simplicity.

In terms of this basis (and noting the above reservations), we can construct the $(n_I + n_{\bar{I}}) \times (n_I + n_{\bar{I}})$ matrix $D = h \bar{\partial} j_i$ which has block zeroes on the diagonal and $V; V^Y$ on block diagonal. There is however a fundamental objection to D being thought of as a matrix representation of the Dirac operator $\bar{\partial} [A]$. This is due to the fact that the basis we

have chosen is not orthonormal;

$$\begin{aligned}
 h_{i,j}^+ j_{j,i}^+ i &= U(x_i^+; i^+; x_j^+; j^+) \\
 h_{i,j}^- j_{j,i}^- i &= U(x_i^-; i^-; x_j^-; j^-) \\
 h_{i,j}^- j_{j,i}^+ i &= 0; \tag{7}
 \end{aligned}$$

hence the matrix D is simply not a representation. (We have again ignored the possible dependence of the matrix element on the relative colour orientation of the objects; this is again for simplicity.) We can however construct an orthonormal basis $f_j e^+ i; j e^- i$ using the standard Gram-Schmidt procedure,

$$\begin{aligned}
 j_{j,i}^+ i &= R_{ij} j_{i,i}^+ i \quad 1 \quad j \quad i \quad n_{\bar{i}} \\
 j_{j,i}^- i &= S_{ij} j_{i,i}^- i \quad 1 \quad j \quad i \quad n_i; \tag{8}
 \end{aligned}$$

It is easy to see that in terms of this new orthonormal basis, a matrix representation of the Dirac operator is given by:

$$\begin{aligned}
 \not{D} &:= \not{D} = \begin{pmatrix} 0 & z_{\bar{i}} \not{\sigma}_1^{\bar{i}} \not{\sigma}_1^i \{ & z_{\bar{i}} \not{\sigma}_1^{\bar{i}} \not{\sigma}_1^i \{ & 1 & 0 \\ h_{i,i}^+ \not{\sigma}_1^i \not{\sigma}_1^j j_{j,i}^+ i = 0 & h_{i,i}^+ \not{\sigma}_1^i \not{\sigma}_1^j j_{j,i}^- i = \not{\nabla}_{ij}^C & A & 0 & n_{\bar{i}} \\ h_{i,i}^- \not{\sigma}_1^i \not{\sigma}_1^j j_{j,i}^+ i = \not{\nabla}_{ij}^V & h_{i,i}^- \not{\sigma}_1^i \not{\sigma}_1^j j_{j,i}^- i = 0 & & & n_i \end{pmatrix} \tag{9}
 \end{aligned}$$

where

$$\not{\nabla} = (R^{-1})^V V S^{-1} \tag{10}$$

We see that this orthonormalization procedure preserves the chiral properties of the original wavefunctions; ${}^5 j^e i = j^e i$. This matrix representation fulfills many of the requirements for the Dirac operator. It is easy to see that the elements of the matrices R ; S and D are not random; they obey various triangle inequalities as they are given by overlap integrals between wavefunctions. Gram-Schmidt orthonormalization would be impossible for a general matrix without this property. It is also easy to see that \not{D} satisfies the 5 symmetry; all non-zero eigenvalues come in pairs. Furthermore we see that the Atiyah-Singer theorem

is obeyed; any configuration has at least $\int_{I^+} \int_{I^-}$ exact zero eigenvalues. If we consider the case of a single $I^+ \cap I^-$ pair (so orthonormalization becomes trivial), then it is easy to see that by choosing the function V appropriately, we can recover the correct eigenvalue splitting. (This is given by the overlap matrix element between would-be zero mode wavefunctions.) All these features give us reason to believe that our toy model should capture the essential features of the mechanism whereby eigenvalues are split from zero.

All we have to decide is what form of trial would-be zero mode wavefunction to use for our objects. Simple examples include the hard sphere, Gaussian and classical zero mode wavefunctions. It is of course not possible to say which wavefunction will dominate the quantum vacuum. In this paper we concentrate on the simplest possible case, that of hard sphere wavefunctions;

$$\begin{aligned} h(x_j) &= 1 & j &= x_j & j < & j \\ &= 0 & \text{otherwise:} & & & \end{aligned} \quad (11)$$

This choice would of course lead to an artificially singular form for V_{ij} and so (again in the interests of simplicity) we replace the derivative with $1 = \frac{p}{1 - 2}$ so that both U and V are modeled by hard sphere wavefunctions but with the correct dimensions. We leave it to another publication to investigate more closely the universality of our results [10] for different wavefunction choices. It suffices to say that the only features which can be considered to be of significance are those which are largely independent of the trial wavefunction used. It is only these features which we can hope will survive in the quenched QCD vacuum.

Each configuration in the ensemble consists of a set of positions, sizes and winding numbers (\mathbf{l}) which label the objects in the vacuum. This set is either extracted from gauge field configurations generated by UKQCD [3] or alternatively, produced by a model that simply generates them at random. The advantage of the former method is that it may give a more accurate description of the topological content of the quenched QCD vacuum; the latter method has the advantage that we can obtain far higher statistics. And in some sense it isolates more cleanly the physics due to instantons, since the instantons in the lattice

elds certainly contain correlations which are due to other dynamics. We use the method outlined above to find the low lying eigenvalues for each given configuration. These are then used to generate the spectral density.

III. RESULTS

In [3] SU(3) lattice gauge field configurations of sizes $16^3 \times 48$ at $\beta = 6.0$, $24^3 \times 48$ at $\beta = 6.2$ and $32^3 \times 64$ at $\beta = 6.4$ were cooled and the corresponding instanton ensembles extracted for various numbers of cooling sweeps. Over this range of $\beta = 6.0 \rightarrow 6.4$ the lattice spacing varies by a little less than a factor of 2 and these three volumes are approximately the same in physical units. Comparing the results at the three values of β enables the approach to the continuum limit to be studied. Of course, instantons can be large and it is important to control finite volume effects as well. For this purpose calculations were also performed at $\beta = 6.0$ on a much larger $32^3 \times 64$ lattice. The conclusion was that finite volume corrections were negligible and that there was good scaling of, for example, the instanton size distribution, if one varied the number of cooling sweeps with β so as to keep the average number of instantons constant. Some properties of these lattice configurations are listed in Table I.

In this section we shall take these configurations, ranging in number from 20 to 100 depending on the lattice size and the value of β , and we calculate the spectral density of the would-be zero modes as described in the previous section. We shall, for simplicity, not employ some of the rather complicated procedures used in [3] for filtering out possible false instanton assignments. Rather we shall take the raw instanton ensembles, after correcting as in [3] for the influence of the instantons upon each other, without applying any further filter. (Except that we throw away any charges that are larger than the volume available. This usually involves rejecting (much) less than 1% of the total number.) In addition, we calculate the size from the (corrected) peak height. We are confident that the results we obtain from these ensembles differ very little from the results we would have obtained using the slightly different ensembles obtained by applying the more complex procedures of [3].

There are several questions we wish to address. These include:

Does a realistic ensemble of instantons break chiral symmetry spontaneously? Lattice calculations find that it does; but the presence of important lattice artefacts renders the conclusion suspect. Continuum calculations using model ensembles of instantons also find that they break chiral symmetry; but it is not clear that the real world is like the model.

Is the spectral density of quenched QCD pathological? Some model calculations have found that the spectrum appears to diverges at $\tau = 0$ [11,12,15]. Whether this is related to the recent discussion, within quenched chiral perturbation theory, of a logarithmic divergence is also of interest [15,16].

Do fermionic physical observables, such as the chiral condensate or spectral density, also exhibit scaling and small finite volume corrections?

Do fermionic physical observables, such as the chiral condensate, exhibit a weak variation with cooling, implying that the rapid variation of the instanton ensemble that one observes is only apparent rather than real?

Figure 1 shows the spectral density that results from the 51 configurations generated after 46 cooling sweeps on the $32^3 64$ lattice at $\tau = 6.0$. We see a pronounced peak as $\tau \rightarrow 0$, just like the divergence that characterises model instanton ensembles. (Note that the exact zero modes contribute an invisible δ -function. Because this should be regarded as a finite volume effect, we shall disregard it.) What is the functional form of this peak? We first attempt to model it via a simple log divergence $\rho(\tau) = a + b \log(\tau)$. This gives a fairly good fit as can be seen in figure 2 where it would correspond to a straight line. However a fit to $\rho(\tau) = c \tau^n$, as shown in figure 3 where it would again correspond to a straight line, gives an equally good (if not better) fit. As we shall see below, we have found in general that the strength of this peak decreases as the density of objects increases (also see [10,12]). The fact that we still see any peak whatsoever when dealing with such a dense gas of objects (see Table I), gives us evidence that a divergence as $\tau \rightarrow 0$ is a generic feature of instanton ensembles in practice. We do not quote the actual powers of the divergence as these are non-universal quantities, the fact that there is a divergence however does appear to

be universal [10,12]. The quark condensate as a function of quark mass is given in figure 4. We already know that this order parameter must vanish for very small quark masses because of the gap in the eigenvalue spectrum (we cannot take the quark mass to zero in a finite box). Extrapolating to zero quark mass (whilst ignoring the dip at small quark masses), we find that chiral symmetry is broken with an order parameter $h^- \approx (400 \text{ MeV})^3$. Whilst this is larger than the phenomenological figure, $h^- \approx (300 \text{ MeV})^3$, it is surprisingly close considering the toy model nature of our calculations. The fact it is larger however, is a reflection of the high density of this gas of instantons.

We can also ask whether it makes a difference if we position the objects at random, as opposed to their true lattice locations. Figure 5 shows that indeed it does. We find (in all cases that we tested) that the spectral density increases at small eigenvalues if the objects are positioned at random (and conversely decreases at larger eigenvalues). The easiest explanation for this is that we are seeing screening of charges on the lattice; this screening implies that opposite sign charges are closer, and this causes greater eigenvalue splitting than if the charges were distributed at random. This complements the direct observation of screening in [3]. We can also test the effect of only including instantons which are smaller or larger than a certain size. This is shown in figure 6. Here we compare the spectral densities generated by including all objects, objects smaller than the average volume and objects larger than the average volume. We see that interactions between the small objects alone leads to a strongly divergent spectral density and, perhaps more surprisingly, that this is also the case, albeit less dramatically, for the large instantons alone.

Figure 7 and Figure 8 show the spectral density for the 20 configurations generated at $\beta = 6.4$ (corresponding to the smallest lattice spacing) on a $32^3 64$ lattice for different numbers of cooling sweeps. We see something rather surprising; as we cool more, and as we find fewer objects in the same volume, the entire spectral density shifts down proportional to the change in instanton number. This is in contrast to the optimistic expectation that cooling, being a local smoothening, should have less effect at small eigenvalues ('infrared physics') and more effect at large eigenvalues ('ultraviolet physics'); as one might expect if

the main reason for the decrease of the number of charges with cooling was that heavily overlapping objects which produce large eigenvalues were annihilating. This naive hope is seen to be unrealized. It is therefore not surprising that cooling dramatically alters the quark condensate, as can be seen in figure 9. (As usual this plot excludes the exact zero modes which would give a finite-volume peaking of the condensate at small quark masses.) Whilst we should not pay too much attention to the exact figures for the quark condensate (given the qualitative nature of this work), the fact that cooling alters the quark condensate so greatly is of importance. The clear message is that the important fermionic physical observables do vary with cooling and this leaves an ambiguity in calculations of the instanton content of the vacuum that must be resolved.

We see in Figure 7 that there is a pronounced peaking of the spectrum near $\omega = 0$, at least for a small number of cooling sweeps. Figure 10 plots the densities so as to expose a log divergence whilst figure 11 does the same for a power divergence. Once more we find that the power divergence is somewhat better (at least for the fewest cooling sweeps). It is of course debatable whether the spectral density is diverging at all, the fits are rather flat. This is partly explained by the highly dense nature of the gas, even at the largest number of cools (Table I). It is also the case that including non-zero values of the total topological charge Q , will, in a finite volume, deplete the spectrum of small eigenvalues and conceal the presence of an infinite-volume divergence.

The analysis of data extracted from the lattice suffers from the paucity of data available. We are limited not only in the number of configurations but also in the volume of the lattice analysed. To get a better handle on the form of the divergence (if any), we briefly analyse instanton configurations that have been generated artificially by placing all the topological charges at random positions in space-time [11,12,10]. All these configurations have zero topological charge since we know that $Q = V \neq 0$ as $V \neq 1$, so we expect that taking only $Q = 0$ minimises finite volume corrections. In figure 12 we see how the spectral density changes with the packing fraction. This is defined as the average number of topological charges multiplied by their average volume and divided by the total volume of space-time.

It is a measure of the fraction of spacetime that would be occupied by the objects if they were non-overlapping: increasing the packing fraction whilst holding other variables constant increases the density of objects. We vary the packing fraction from 0.3 to 2.5 for ensembles consisting of a 100000 configurations i.e. from a moderately dilute gas to a dense gas. In all three cases we see a divergence as $\epsilon \rightarrow 0$. We can also try to determine the functional form of the divergence: a log-linear plot is shown in figure 13, whilst a log-log plot is shown in figure 14. We see that a power law gives a far better fit to the divergence for all but the densest ensemble. In this last case, the peak is weakest and so it is no surprise that a logarithmic form works equally well. After all

$$c \sim c + c \log \epsilon \quad (12)$$

for small values of the exponent c . We also see that the power of the divergence decreases as the density of objects increases. This fits in with the intuitive picture whereby a higher packing fraction leads to greater splitting hence a weaker divergence (if any). This may also help to explain why the divergence seen in the actual lattice data is so weak; the packing fraction is greater still. For a much more detailed model analysis, see [12,10].

Returning to the lattice instanton ensembles, another question we want to ask is whether the finite volume corrections are really under as good a control as they appear to be if one focuses on simple gluonic observables such as the density of instantons and the size distribution [3]. For this purpose we display in figure 15 the spectral densities that one obtains after 46 cools from the $16^3 48$ and $32^3 64$ lattices at $\beta = 6.4$. We observe that they are entirely similar, even down to the details of the forward peak. This shows that at least for these parameters any finite volume corrections are negligible.

Of course $\beta = 6.0$ corresponds to our coarsest lattice, and it would be nice to have a similar study closer to the continuum limit, say at $\beta = 6.4$. Unfortunately that would require lattices much larger than $32^3 64$ which is clearly impractical. By contrast, a nice feature of using our model is that it is easy to increase the volume and so test whether one has reached the infinite volume limit. We show the results of such a calculation in figure 16.

We compare the spectral densities generated from random configurations at a constant value of the packing fraction and for three volumes that vary by about a factor of 3. The packing fraction has been chosen to equal that of the instanton ensemble that one obtains after 80 cooling sweeps from the fields generated at $\beta = 6.4$ on the $32^3 64$ lattice; and the middle of the three volumes has been chosen to be close to that of the lattice. The lattice and model ensembles differ in that the latter contain objects of a single size positioned at random and with a total charge that is always zero, $Q = 0$. The spectral density obtained from the lattice ensemble is also shown. We observe that the model spectra compare quite well with the lattice spectrum. One difference is that the lattice spectrum lacks a forward peak but we have already remarked that this is in part due to the fact that the model ensemble always has $Q = 0$ while the lattice configurations typically have quite large values of $Q \neq 0$. We note from the figure that the larger two of the three volumes produce essentially identical (model) spectra. Thus the $V \rightarrow 1$ limit appears to be readily accessible.

Finally we address the question of scaling. In [3] it was shown that if we vary the number of cooling sweeps with β appropriately, then many properties of the instanton ensemble become independent of β once they are expressed in physical units. Is this also true of the more subtle features that are embodied in physical observables such as the chiral condensate? To investigate this we plot in figure 17 the spectral densities obtained after 23, 46 and 80 cooling sweeps on the $16^3 48$, $24^3 48$ and $32^3 64$ lattices at $\beta = 6.0; 6.2; 6.4$ respectively. These lattices have nearly equal volumes in physical units and the variation with β of the number of cooling sweeps is as prescribed in [3]. As we see the corresponding spectral densities are very similar showing that the important fermionic physical observables do indeed scale.

IV. CONCLUSIONS

We have seen evidence that the spectral density diverges as $\beta \rightarrow 0$ in quenched QCD. The analysis was based on instanton ensembles derived from Monte Carlo generated lattice field configurations and was supplemented by ensembles of instantons generated by a model

that placed them at random on the hypertorus. This divergence follows an approximate power law, $/ \sim n$, and n increases as the density of objects decreases. This indicates that such a divergence is ubiquitous if we deal with instanton ensembles. It should be noted that this divergence has also been seen by unfolding the microscopic spectral density obtained via Random Matrix Theory [15]. In that paper it was suggested that the divergence was logarithmic as expected from recent quenched chiral perturbation theory arguments [16]. Although in some cases our results are also consistent with a logarithmic divergence this only happens when the exponent n is so small that it is presumably a trivial consequence of equation (12).

We have furthermore found evidence, from a comparison of the Dirac spectral densities, for some of the claims in [3]: in particular for the screening of topological charges in the quenched QCD vacuum, for the smallness of finite volume corrections and for the claim that if the number of cooling sweeps is varied with β so that the number of topological charges per unit physical volume is constant, then the physical observables show scaling.

However we have also found that fermionic physical observables such as the chiral condensate vary strongly with the number of cooling sweeps. This means that one must learn how to factor out the effects of cooling before one can claim to have completely understood the true instanton structure of the gauge theory vacuum.

V. ACKNOWLEDGEMENTS

The lattice instanton ensembles used in this work were produced by Douglas Smith and one of the present authors (MT). They were derived from gauge field configurations produced by UKQCD. We are grateful for this material. One of us (US) wishes to thank PPARC for financial support (research studentship number 96314624). The computations herein were performed on our departmental workstations. We are grateful to PPARC for support under PPARC grant GR/K 55752.

REFERENCES

[1] C. Michael and P. Spencer, *Phys. Rev. D* 52 (1995) 4691;
Ph. de Forcrand, M. Garcia Perez and I-O Stamatescu, *Nucl. Phys. B* 499 (1997) 409;
T. DeGrand, A. Hasenfratz and T. Kovacs, *Nucl. Phys. B* 505 (1997) 417; *B* 520 (1998)
301.

[2] Ph. de Forcrand, M. Garcia Perez, J. Hetrick and I-O Stamatescu, *hep-lat/9802017*;
A. Hasenfratz and C. Nieder, *hep-lat/9806026*.

[3] D. A. Smith and M. Teper, *Phys. Rev. D* 58 (1998) 014505.

[4] T. Schafer and E. Shuryak, *Rev. Mod. Phys.* 70 (1998) 323.

[5] D. D. Iakonov, *hep-ph/9602375*, Varenna Lectures.

[6] D. Calli, *Phys. Rev. Lett.* 39 (1977) 121;
C. Callan, R. Dashen and D. Gross, *Phys. Rev. D* 17 (1978) 2717;
R. Carlitz and D. Creamer, *Ann. Phys. (N.Y.)* 118 (1979) 429.

[7] M. Teper, Newton Inst. NATO-ASI School Lectures, July 1997, *hep-lat/9711011*.

[8] S. J. Hands and M. Teper, *Nucl. Phys. B* 347 (1990) 819.

[9] R. Edwards, U. Heller and R. Narayanan, *hep-lat/9811030*;
P. Chen et al, *hep-lat/9811013*;
P. Niedermeyer, *hep-lat/9810026*.

[10] U. Sharan and M. Teper, in preparation.

[11] N. Dowrick and M. Teper, *Nucl. Phys. (Proc. Suppl.) B* 42 (1995) 237.

[12] U. Sharan and M. Teper, *hep-lat/9808017*.

[13] M. Atiyah and I. Singer, *Ann. Math.* 87 (1968) 484.

[14] T. Banks and A. Casher, *Nucl. Phys. B* 169 (1980) 103.

[15] J. Verbaarschot and J. O. sbom, Nucl. Phys. B 525 (1998) 738.

J. O. sbom, D . Toub lan and J. Verbaarschot, hep-th/9806110.

E . Shuryak, private communication.

[16] M . G olterman, hep-ph/9710468 and private communication.

TABLES

| | $L^3 T$ | Lattice Spacing (fm) | Cools | N_c | $\bar{N}_I = V$ (fm $^{-4}$) | $\bar{N}_I \bar{V}_I = V$ |
|---------------------------|-----------|----------------------|-------|-------|-------------------------------|---------------------------|
| 6.0 | $16^3 48$ | 0.098 | 23 | 100 | 9.1 | 4.2 |
| | | | 46 | 100 | 3.2 | 1.9 |
| 6.0 | $32^3 64$ | 0.098 | 46 | 51 | 3.5 | 2.8 |
| 6.0 ($V_I < \bar{V}_I$) | $32^3 64$ | 0.098 | 46 | 51 | 2.4 | 0.8 |
| 6.0 ($V_I > \bar{V}_I$) | $32^3 64$ | 0.098 | 46 | 51 | 1.2 | 2.0 |
| 6.2 | $24^3 48$ | 0.072 | 46 | 100 | 8.9 | 4.9 |
| 6.4 | $32^3 64$ | 0.0545 | 30 | 20 | 56.6 | 12.4 |
| | | | 50 | 20 | 21.7 | 8.5 |
| | | | 80 | 20 | 9.2 | 5.3 |

TABLE I. Some information about the data analysed in this paper. V is the total space-time volume, \bar{V}_I is the average volume of an instanton in the ensemble, \bar{N}_I is the average number of topological charges per configuration and N_c is the number of configurations in the ensemble.

FIGURES

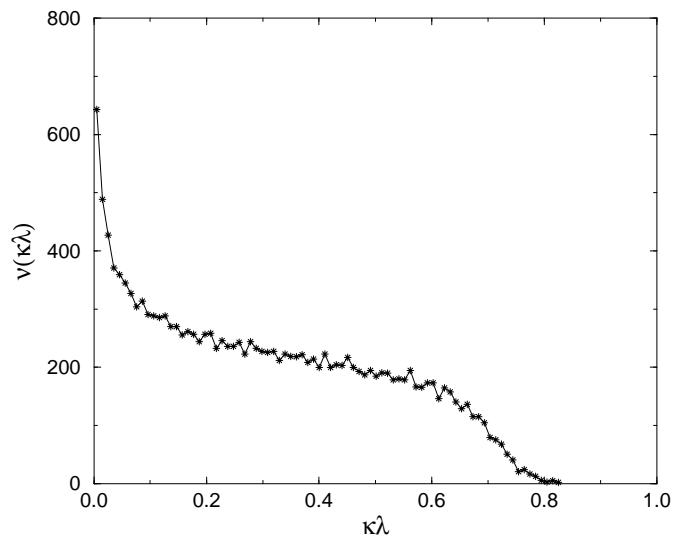


FIG. 1. The spectral density: $\epsilon = 6.0$; $32^3 64$; 51 configurations. The eigenvalues are scaled for convenience by $\epsilon = (2\bar{V}_I)^{1/4}$, a measure of the average instanton size.

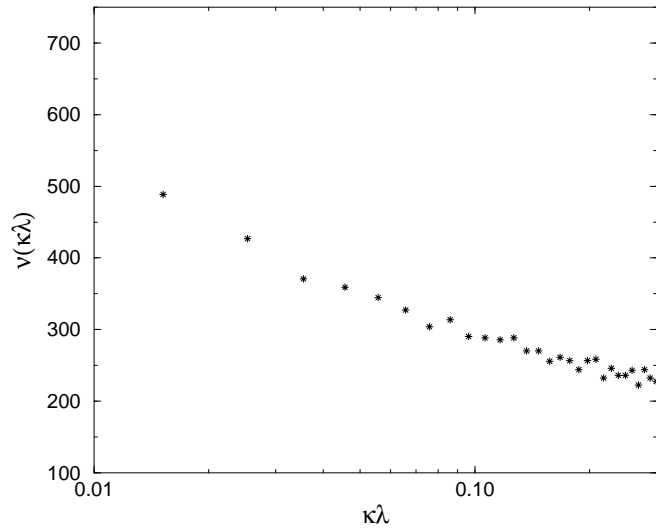


FIG. 2. The spectral density in figure 1, plotted on log-linear axes.

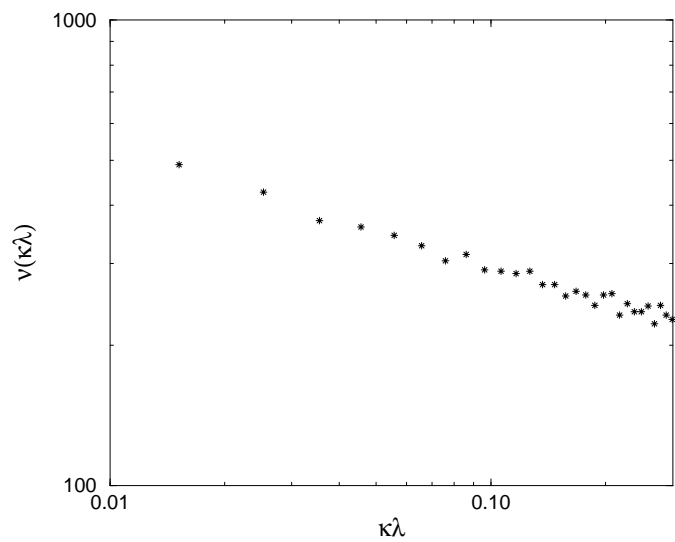


FIG. 3. The spectral density in figure 1, plotted on log-log axes.

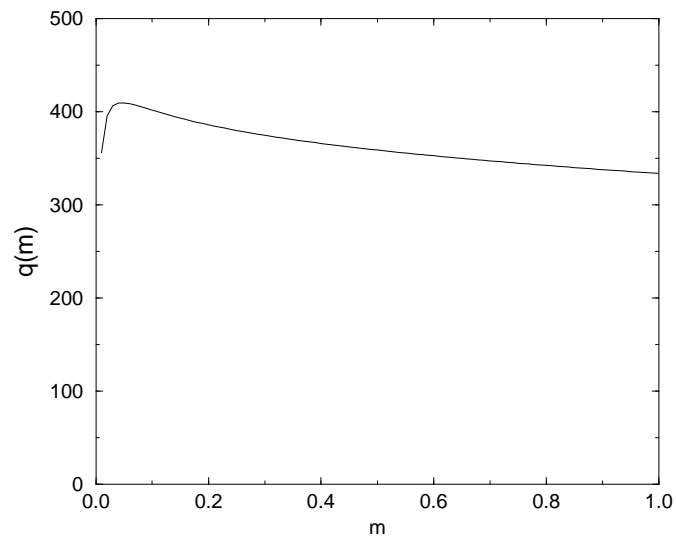


FIG. 4. $h̄(m) = (q(m)M \text{ eV})^3$ as obtained from the spectral density in figure 1.

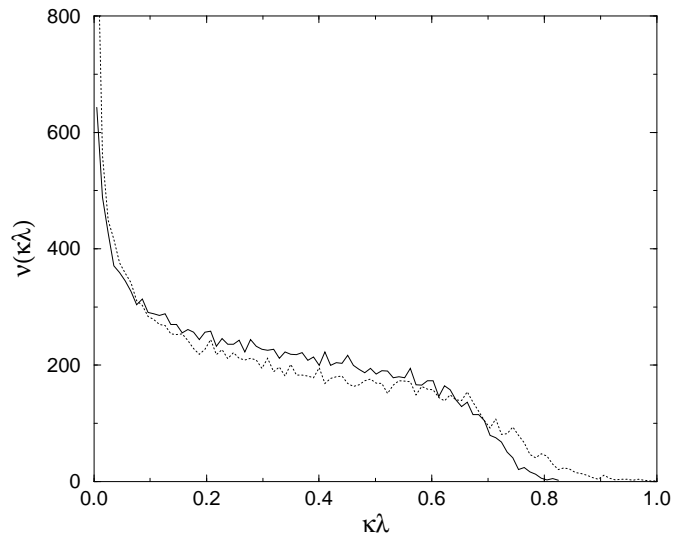


FIG. 5. The spectral density of figure 1 (solid), compared to the density obtained by positioning the same charges at random (dotted).

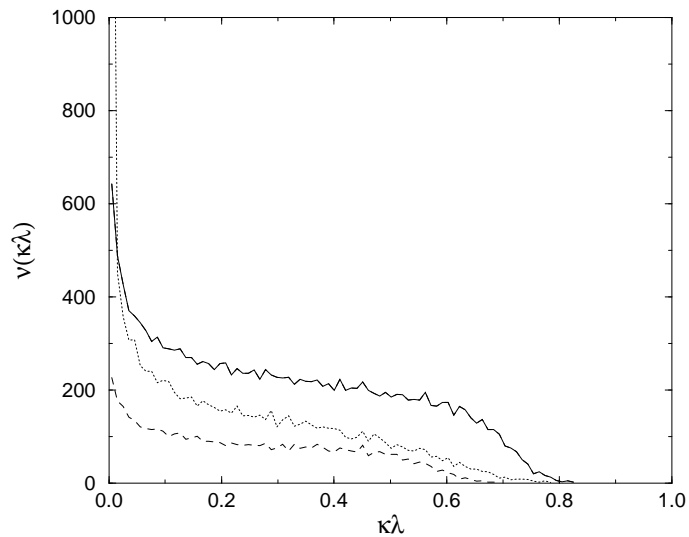


FIG. 6. The spectral density in figure 1 (solid) compared to the densities obtained by separating the instantons into those with volumes smaller/larger than the average (dotted/dashed).

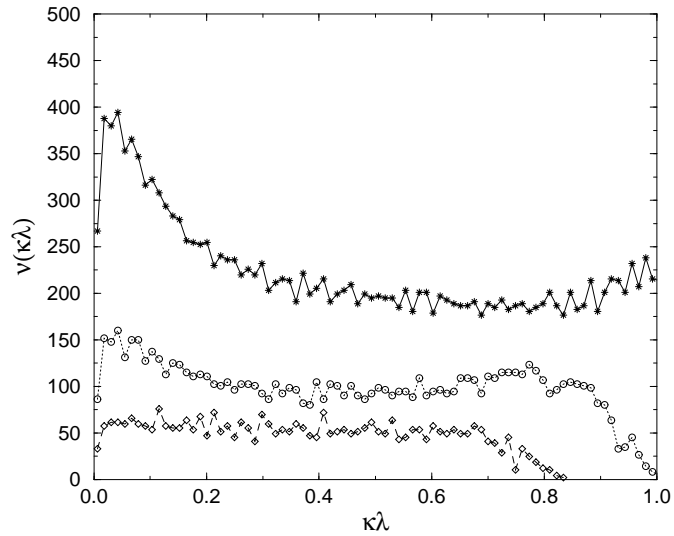


FIG . 7. The spectral densities obtained from the $\epsilon = 6:4$; $32^3 64$ configurations for various numbers of cooling sweeps: ? 30 cools, 50 cools, 3 80 cools. Here the ϵ is from 50 cools.

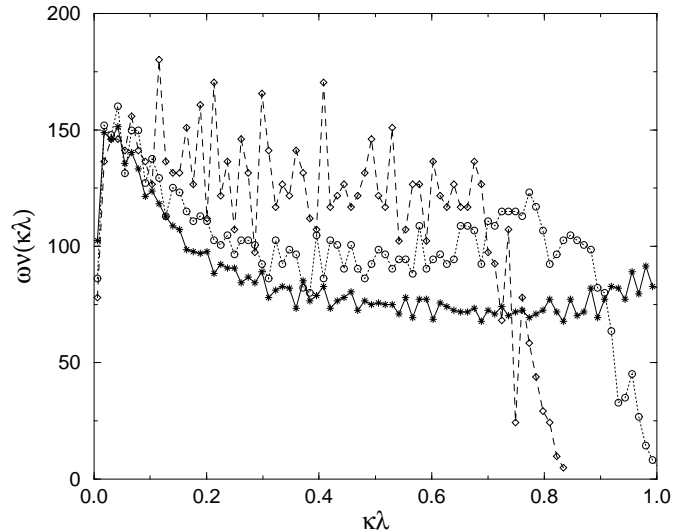


FIG . 8. The same densities as in figure 7 but rescaled by $\epsilon = n_{50}/n_i$, where n_i is number of objects after i cooling sweeps.

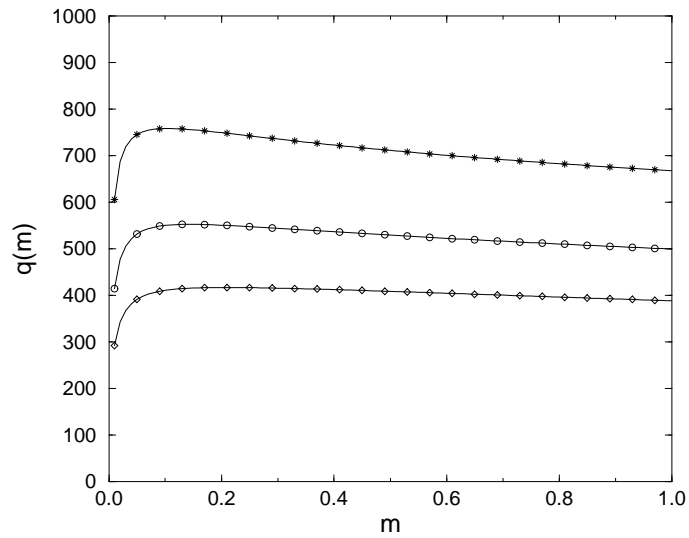


FIG. 9. $h_i = (q(m)M \text{ eV})^3$ obtained from the spectral densities in figure 7.

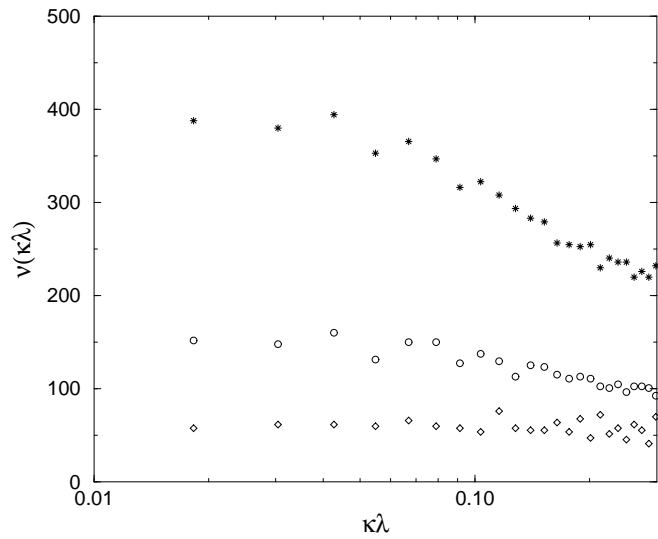


FIG. 10. The spectral densities in figure 7, plotted on log-linear axes.

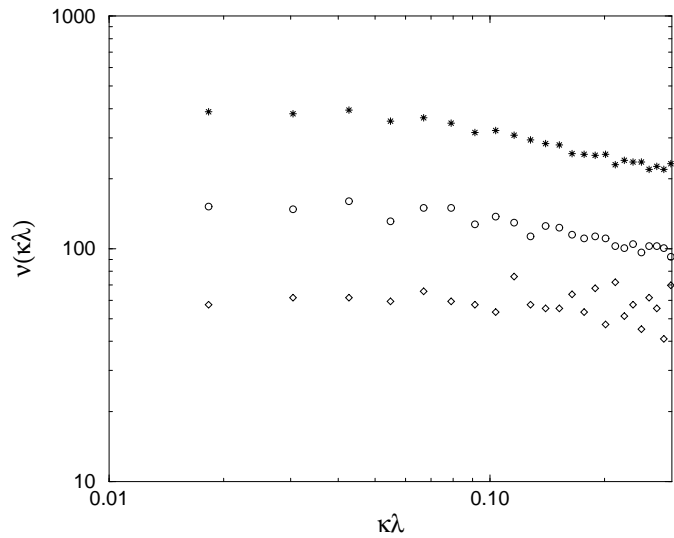


FIG .11. The spectral densities in figure 7, plotted on log-log axes.

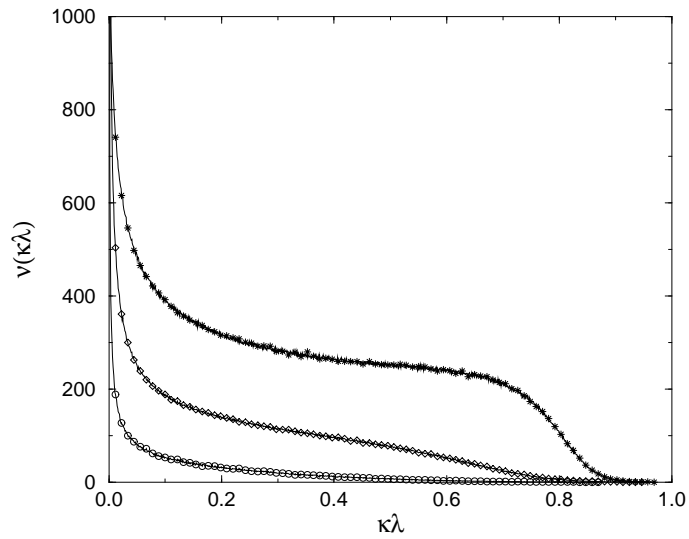


FIG .12. Spectral densities from configurations generated by the random position model, for various packing fractions: $N \bar{V}_I = L^4 = 0.3$ ($N = 19 + \bar{19}$), 1.0 ($N = 63 + \bar{63}$) & 2.5 ($N = 153 + \bar{153}$).

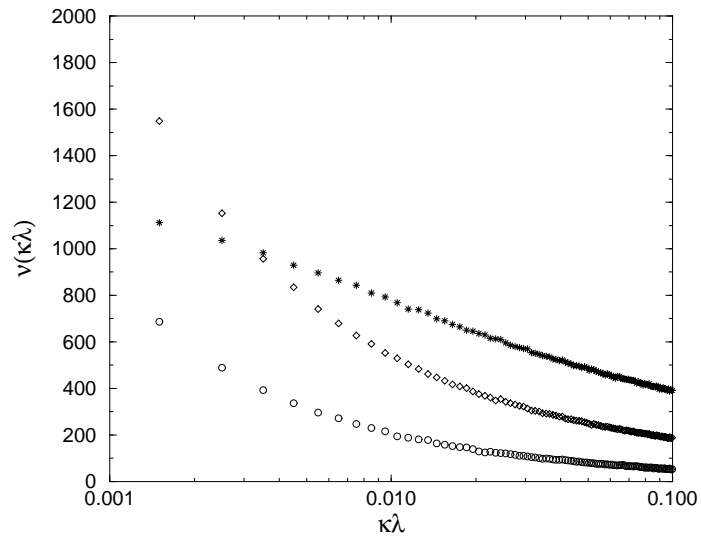


FIG. 13. Spectral densities in figure (12), plotted on log-lin axes.

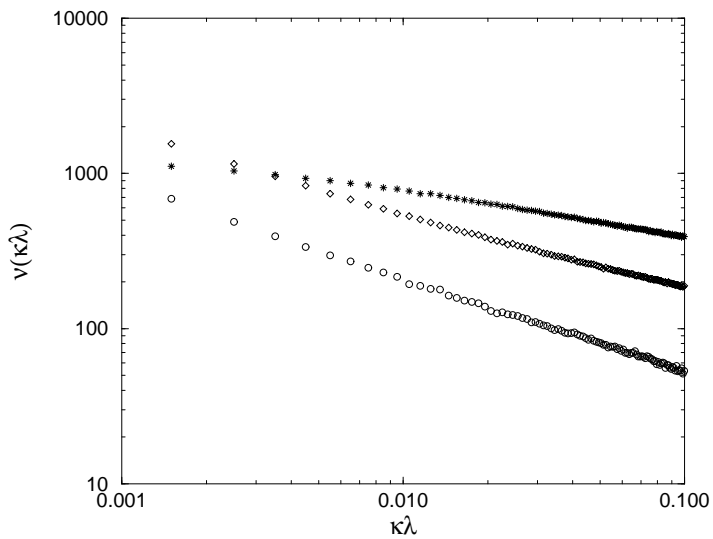


FIG. 14. Spectral densities in figure (12), plotted on log-log axes.

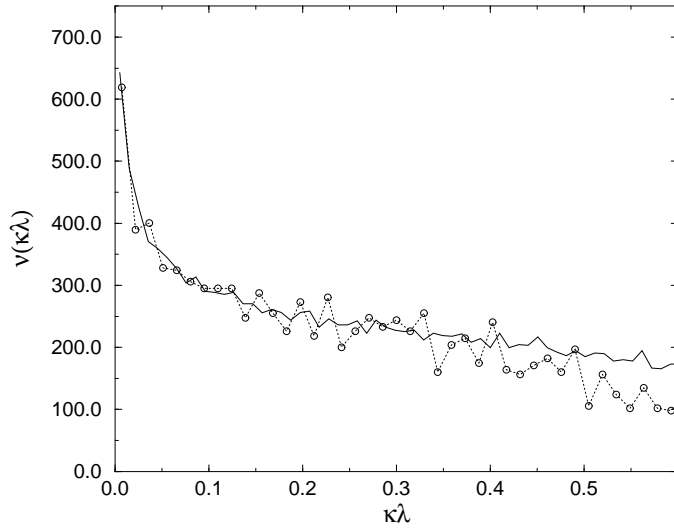


FIG. 15. Spectral densities from two different volumes at $\beta = 6.0$, after 46 cooling sweeps: $32^3 64$ (solid) and $16^3 48$ (dashed) lattices.

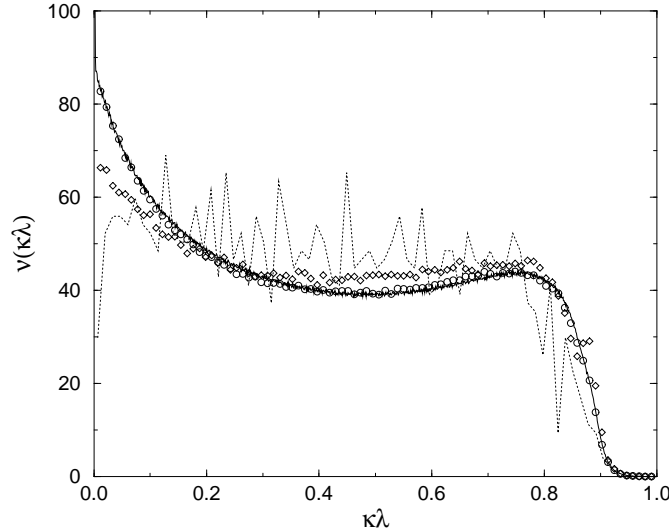


FIG. 16. Spectral densities from configurations with instantons of equal size placed at random, on three different volumes: $\overline{N}_I \overline{V}_I = V = 4.88$, $V = 1$ (), $V = 2.29$ () and $V = 3.03$ (solid line). Compared to the spectral density from the lattice fields at $\beta = 6.4$ after 80 cools (dashed line), which corresponds to $\overline{N}_I \overline{V}_I = V = 4.88$ and $V = 2$. Here is from 80 cools.

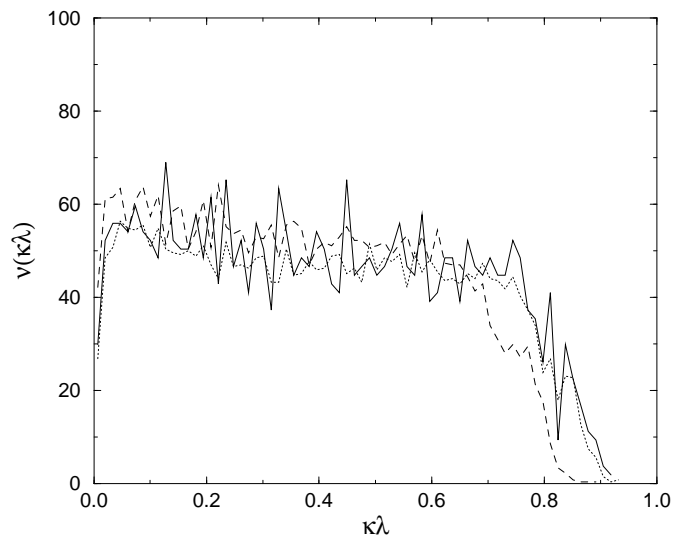


FIG. 17. The spectral densities obtained at $\tau = 6.0; 6.2; 6.4$ after 23, 46, 80 cooling sweeps respectively. All in physical units, with τ from $\tau = 6.4$.